NANO LETTERS

pubs.acs.org/NanoLett

Letter

Electron Beam Maneuvering of a Single Polymer Layer for Reversible 3D Self-Assembly

Chunhui Dai and Jeong-Hyun Cho*

Cite This: *Nano Lett.* 2021, 21, 2066−2073

Read Online

ACCESS | Metrics & More | Article Recommendations | Supporting Information

ABSTRACT: Reversible self-assembly that allows materials to switch between structural configurations has triggered innovation in various applications, especially for reconfigurable devices and robotics. However, reversible motion with nanoscale controllability remains challenging. This paper introduces a reversible self-assembly using stress generated by electron irradiation triggered degradation (shrinkage) of a single polymer layer. The peak position of the absorbed energy along the depth of a polymer layer can be modified by tuning the electron energy; the peak absorption location controls the position of the shrinkage generating stress along the depth of the polymer layer. The stress gradient can shift between the top and bottom surface of the polymer by repeatedly tuning the irradiation location at the nanoscale and the electron beam voltage, resulting in reversible motion. This reversible self-assembly process paves the path for the innovation of small-scale machines and reconfigurable functional devices.

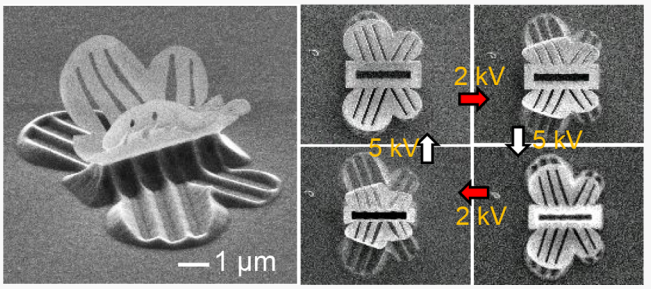

KEYWORDS: *reversible self-assembly, nanoscale locomotion, polymer, 3D, in situ*

Reversible self-assembly is a powerful technique that allows structure transforms between two or more configurations in response to external applied stimuli such as thermal energy,[1] mechanical force,[2,3] electric signal,[4] solvent,[5,6] and light.[7,8] Various applications have been developed based on this process, especially for reconfigurable devices[1−3,8] and robotics.[4−6,9] Reversible alterations of a structure's geometry directly tune its properties, leading to reconfigurable devices. For instance, reconfigurable metamaterials with switchable response frequencies are achieved via folding, unfolding, and refolding of the structures.[1,2] The reversible deformation also aligns perfectly with the needs of reciprocating motion in robotics. Miskin et al. recently reported a microscopic robot based on voltage controlled reversible self-folding of platinum/graphene bilayers.[9] Despite great achievements, it is difficult to utilize the current strategies, which trigger material deformation with large scale stimuli and monitor self-assembly status with microscopes, to realize well-controlled dynamic motion at nanoscale (at most a few tens of micrometers) resolution.

Energetic irradiation (i.e., ion or electron) triggered assembly is a promising solution due to its capability for precisely tailoring the nanoscale deformation of one-dimensional (1D)[10,11] or two-dimensional (2D) structures.[12−18] Owing to a wealth of physical interaction between energetic irradiation and materials, stress-induced nanoscale deformation as well as imaging of a structure can be simultaneously achieved in an ion/electron beam system, leading to in situ monitored self-assembly. In addition, the tunability of the beam enables accurate delivery of ions/electrons to a specific spot with required irradiation energy. These combined advantages create a controllable and programmable assembly technique.[19,20] Compared to conventional invisible self-assembly techniques,[21,22] the in situ monitored assembly process enables realization of 3D architecture with nanoscale precision and much more complexity.[19] Furthermore, by incorporating advanced designs into the self-assembled architectures, the assembled structures can be enhanced with advanced functions such as toroidal excitation,[23] chirality,[24,25] surface adhesion,[26] and plasmonic sensing.[20] The nanoscale controllable stimuli, real-time imaging, and integration with functional materials make the ion/electron beam techniques an ideal platform for reversible self-assembly of reconfigurable devices or robotics. Previous work demonstrated the reversible actuation in graphene/poly(methyl methacrylate) (PMMA) bilayer by combining e-beam irradiation triggered deformation and spontaneous or heat induced relaxation.[27,28] But, the relaxation mechanism is still not compatible with the electron or ion beam techniques due to lack of control in the recovery process of microscale and further nanoscale structures. A theoretical study proposed a strategy to control mass transport

Received: November 29, 2020
Revised: February 18, 2021
Published: February 25, 2021

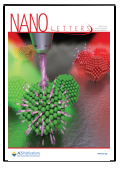

https://dx.doi.org/10.1021/acs.nanolett.0c04723
Nano Lett. 2021, 21, 2066−2073

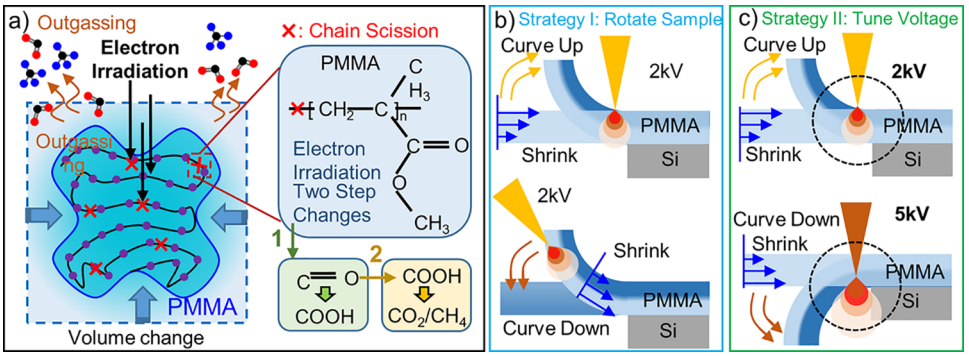

Figure 1. Conceptual schematics showing electron irradiation-triggered PMMA reactions and two strategies of reversible self-assembly. (a) Electron irradiation induces shrinkage of PMMA as a result of the chain scission and outgassing. By (b) rotating the sample or (c) tuning the electron beam voltage, the shrinkage location can be precisely controlled, leading to reversible self-folding.

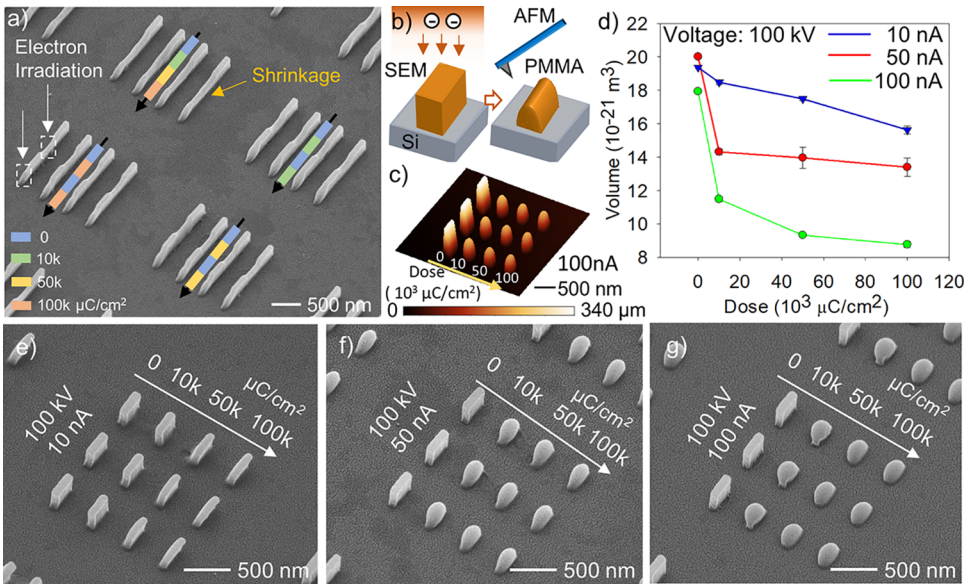

Figure 2. Analysis and characterization of electron interaction with PMMA. (a) SEM image showing the electron irradiation-induced localized shrinkage in PMMA patterns. (b) Schematics, (c) AFM 3D image, and (d) plot showing the measurement of PMMA pillar volume change with different irradiation doses. (e–g) PMMA pillars irradiated by electron beam with the beam current of (e) 10, (f) 50, and (g) 100 nA. The dose is varied between 0, 10k, 50k, and 100k μC/cm^2. Each irradiated segment in panels a, e, f, and g is a 400 × 150 nm square.

in the thin film by manipulating the incident ion energy and flux, which can further tune the deformation direction.[29] However, because of the significant physical damage during ion irradiation, the controllable deformation direction can hardly be experimentally demonstrated, and the reversible process remains impossible.

Here, we developed an approach to achieve reversible self-assembly with nanoscale controllability using electron beam (e-beam) irradiation in a scanning electron microscope (SEM). Under electron irradiation, PMMA exhibits significant shrinkage. The extent of shrinkage relies on the localized electron irradiation profile and absorbed energy distribution, which generates a stress gradient within the homogeneous PMMA film. The stress gradient curves the 2D film up or down, transforming it into a 3D structure. The stress gradient is modified by tuning electron irradiation voltages, allowing a peak stress to move between top and bottom surfaces. The peak stress position in the PMMA thin film determines the deformation direction, leading to reversible self-assembly. The position control can be achieved with nanoscale resolution thanks to the real-time imaging capability of a SEM.

The basic concept of the self-assembly originates from volume changes induced by electron irradiation. A SEM offers electron irradiation precisely controlled with a nanoscale resolution, which can trigger rich and complex chemical and physical reactions in irradiated materials. PMMA has been chosen as the target material because it is one of the most widely used e-beam resists, and its processing parameters are well-established. In response to low irradiation energy, cross-linking (gelling) and scission (degradation) occurs in the resist, but the scission is much more dominant.[30] The absorbed energy can accumulate through migration along polymer chains and be sufficient to break the bonds, resulting in chain scission.[30] Electron irradiation-induced PMMA degradation occurs in two steps. First, the side chains are removed by implanted electrons. Next, the principal chain scissions occur with further irradiation.[31] As a result of chain scission, a vast amount of decomposition gases is generated and emitted from the PMMA in a process called outgassing. For example, the C═O units of pendant polymer chain first decompose into COOH and then into CO_2 and CH_4[32] (Figure 1a). This decomposition has been confirmed by various characterization

https://dx.doi.org/10.1021/acs.nanolett.0c04723
Nano Lett. 2021, 21, 2066−2073

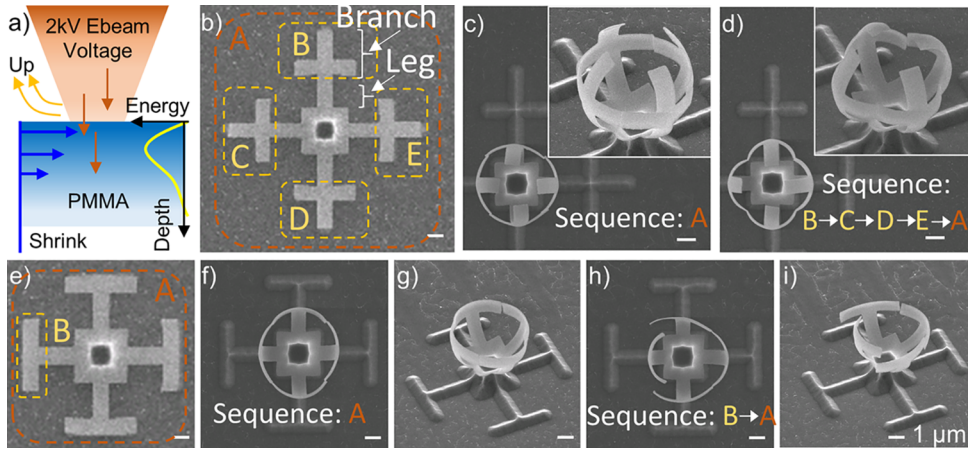

Figure 3. Demonstration of the sequential assembly. (a) The mechanism of self-assembly is based on differential energy absorption in the PMMA thin films. (b) The suspended 2D PMMA pattern is curved into (c) a sphere via universal homogeneous irradiation (A in b). (d) By assigning an additional dose to a specific area (B in b), the topology of the sphere is further modified. (e−i) The symmetry of the assembled structures is tuned by different irradiation sequences, leading to (g) symmetric and (i) asymmetric patterns. For the homogeneous irradiation shown in panels b and e, the SEM imaging magnitude is 5000×, which results in an exposed area of ∼25 × 18 μm. For the localized irradiation (B−E in b and B in e), the exposure area is ∼5 × 3.6 μm.

techniques such as the appearance of a new carboxylic acid peak in the FTIR spectrum.[32] In addition, molecular dynamic simulation has been conducted to theoretically confirm the evolution of the PMMA molecule into gases.[31] Because of the chain scission and consequent outgassing, the PMMA resist exhibits a dramatic volume decrease or shrinkage. The absorbed irradiation energy is the determinant factor of the PMMA shrinkage. The area in the PMMA film that absorbs more irradiation energy exhibits more dramatic shrinkage. Due to the positive correlation between the absorbed irradiation energy and the shrinkage, it is possible to create inhomogeneous shrinkage in the homogeneous thin film based on the intrinsic energy distribution of irradiation, generating a stress gradient along the depth of the PMMA for self-assembly (Figure 1b, c). It should be noted that such a stress gradient can hardly be achieved in single material thin film based on the thermal expansion mechanism that is commonly used for folding bilayer materials with different thermal coefficients. Also, if thermal expansion is the mechanism, under 2 keV irradiation, the top surface should absorb more energy and has a higher temperature, which will expand more than the bottom side, making the structure fold downward. This is contradicted with our observation. In addition, for the thermal expansion caused self-assembly, the deformed structure should return to its original flat status once the heat source is removed, which is also not observed in our case. Based on this information, the thermal expansion mechanism is ruled out. Furthermore, the controllable e-beam offers the capability to precisely tune the depth of peak energy absorbed in the PMMA thin film by changing the irradiation area or the e-beam voltage, allowing for the control of the curving direction and the radius of the curvature. Reversible assembly can be realized through subsequent shrinkage between the top and bottom surface by separately targeting the different surfaces (Figure 1b) or by controlling the position of the peak energy along the depth of the PMMA layer (Figure 1c).

To confirm PMMA shrinkage, 300 nm thick PMMA pillars with a width of 150 nm and a length of 1200 nm were formed on the silicon (Si) wafer through a standard e-beam lithography (EBL) process (Figure 2a) as described in the Supporting Information. Then, the PMMA pillars are irradiated by a second exposure with doses of 0, 10k, 50k, and 100k μC/cm^2 applied to different segments along the long PMMA pillars using an e-beam voltage of 100 kV and current of 50 nA (Figure 2a). The effect of beam current (10, 50, and 100 nA) on morphology and volume of the irradiated PMMA pillars has also been investigated (Figure S1). After the second e-beam exposure, clear volume change is observed between the exposed and unexposed segments, which confirms that electron irradiation induces shrinkage (Figure 2a). Considering the group of pillars that underwent all four doses (Figure 2a top left section), there is a clear trend that a higher dosage produces more significant PMMA shrinkage. The higher beam current also contributes to PMMA deformation (Figure S1).

The relationship between the beam setup (voltage and current) and PMMA shrinkage was quantitatively investigated with the assistance of atomic force microscopy (AFM) (Figure 2b−d). An array of 300 nm thick PMMA pillars with a width of 150 nm and a length of 400 nm was formed on the Si wafer using the aforementioned EBL process, and the PMMA pillars in the array were irradiated with electron streams at different doses (0, 10k, 50k, and 100k μC/cm^2). The e-beam current was also varied between 10, 50, and 100 nA to investigate the influence of currents (Figure 2e−g). After irradiation, the morphology and the volume of the irradiated PMMA pillars were measured (Figure 2c, d). The AFM image of the pillars irradiated by 100 nA e-beam not only show a dramatic volume change (Figure 2d), but also a morphology evolution (Figure 2c). The high density of electrons (due to the higher current) increases the possibility of interaction between electrons and polymer chains, leading to severe chain scissions and reflow. Thus, the edges of the pillars are more degraded as the current (electron density) or beam dose increases, resulting in rounded pillars (Figure 2e−g). It is not surprising to see a positive correlation between the shrinkage and dose. With fixed e-beam voltage and current, higher dose means longer irradiation time, so that more electrons reach the pillars and trigger more considerable chain scission and subsequent outgassing, resulting in more critical shrinkage (Figure 2d). However, irradiations with the same dose do not always result in the

https://dx.doi.org/10.1021/acs.nanolett.0c04723
Nano Lett. 2021, 21, 2066−2073

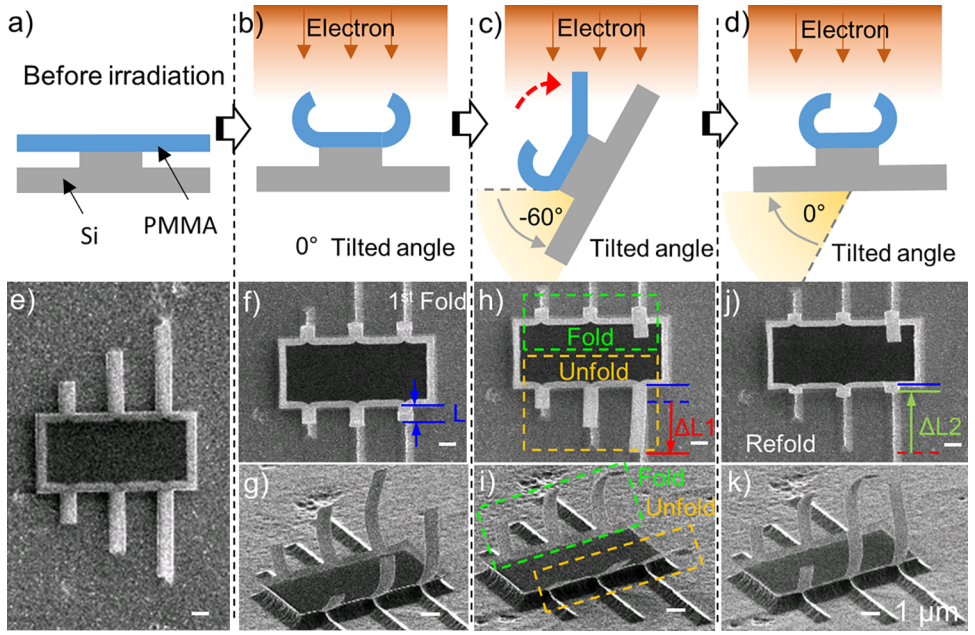

Figure 4. (a–d) Schematics and (e–k) SEM showing the strategy to achieve reversible self-assembly by tilting the substrate. The initial perpendicular irradiation folds the (a, e) 2D suspended cantilevers upward to (b–g) 3D. (c, h, i) Once the substrate is tilted −60°, the bottom side of half of the cantilevers are irradiated, unfolding these cantilevers. (d, j, k) To refold the cantilever upward, the substrate is rotated back to the original state to ensure the perpendicular irradiation. This reversible self-assembly is carried out with the imaging magnitude of 1500×, which leads to an exposure area of ∼75 × 55 μm.

same volume change, as current also plays an important role in determining the shrinkage (the shrinkage is significantly enhanced when the beam current is increased, Figure 2d). This phenomenon originates from the basic mechanism of electron irradiation-induced PMMA shrinkage. Chain scission and subsequent outgassing do not only relay on the energy of a single electron, but also on the total energy that accumulates along the polymer chain within a unit time period.[30] Higher beam current density facilitates the energy accumulation within a unit time, leading to more intense chain scission and subsequent outgassing, which cause considerable shrinkage. It should be noted that volume change caused by sputtering may exist but is not a major component; if it were, the volume change would not saturate at higher irradiation dose, as shown in Figure 2d.

The volume change was utilized for the realization of 3D structures self-assembled in a SEM (Figure 3). A SEM has the ability to simultaneously deliver localized irradiation as a stimulus for assembly and offer real-time imaging to monitor the assembly status,[19] which enables precise manipulation of the assembly behavior and sequence of a structure by programming the irradiation location and order, creating desired 3D architectures. When a homogeneous irradiation is applied at 2 kV to the whole 2D structure (Figure 3a, b, labeled as A), the four legs fold up simultaneously and assemble into a uniform sphere (Figure 3c). Irradiation voltage of 2 kV was selected because the shrinkage occurs in the upper half of the PMMA thin film (a detailed description of irradiation voltages is described in the section of Figure 5). By assigning a sequential irradiation dose to each leg (Figure 3b, labeled as B–E) prior to the homogeneous irradiation (Figure 3b, labeled as A), the three small branches on the leg could be folded up to a desired curvature. It allows precise modification of localized deformation in the structure. Then, homogeneous irradiation is applied to simultaneously fold up the four legs, which makes the four legs fold up together at the same speed and form a closed ring. This homogeneous irradiation assures the alignment of each leg and maintains the symmetry of the self-assembled structure. As a result, the structure is assembled into a deformed sphere with the top view of a clover (Figure 3d). The change of the irradiation sequence can further modify the asymmetry of an assembled structure (Figure 3e–i). By irradiating one leg prior to the other three legs (Figure 3e, labeled as B), the symmetric half sphere (Figure 3f, g) is changed into an asymmetric sphere with two different untouched cambered surfaces (Figure 3h, i). The detailed fabrication process is described in the Supporting Information.

For reversible self-folding (self-curving), two methods are introduced in this paper. The first method involves tilting the substrate holder and monitoring sample conditions in real time in a SEM. The self-folding was made reversible with the assistance of a tilt function by alternating the substrate position so that the irradiation was subsequently directed at the top or bottom surface of the polymer thin film (Figure 4). The 2D suspended cantilevers are first irradiated by an electron stream that is perpendicular to the substrate. As the shrinkage and stress induced in the upper half of the PMMA film (∼−18 nm away from the top of the PMMA layer) with the 2 kV irradiation voltage, all the flat cantilevers (Figure 4a, e) fold upward toward the electron source (Figure 4b, f, g). After that, when the samples are tilted by −60 degrees (Figure 4c), the upper surfaces of the cantilevers on the left of the 2D pattern are still facing the incident electrons, inducing further curvature (Figure 4c, h, i: highlighted in green). However, for the cantilevers on the right side of the patterns, the electrons are irradiated on the bottom surfaces of the cantilevers (Figure 4c). Because of this spatial change, the depth of shrinkage and stress induced is moved to the bottom surface, unfolding the cantilevers (Figure 4h, i: highlighted in orange). When the sample is tilted back to the original position

https://dx.doi.org/10.1021/acs.nanolett.0c04723
Nano Lett. 2021, 21, 2066−2073

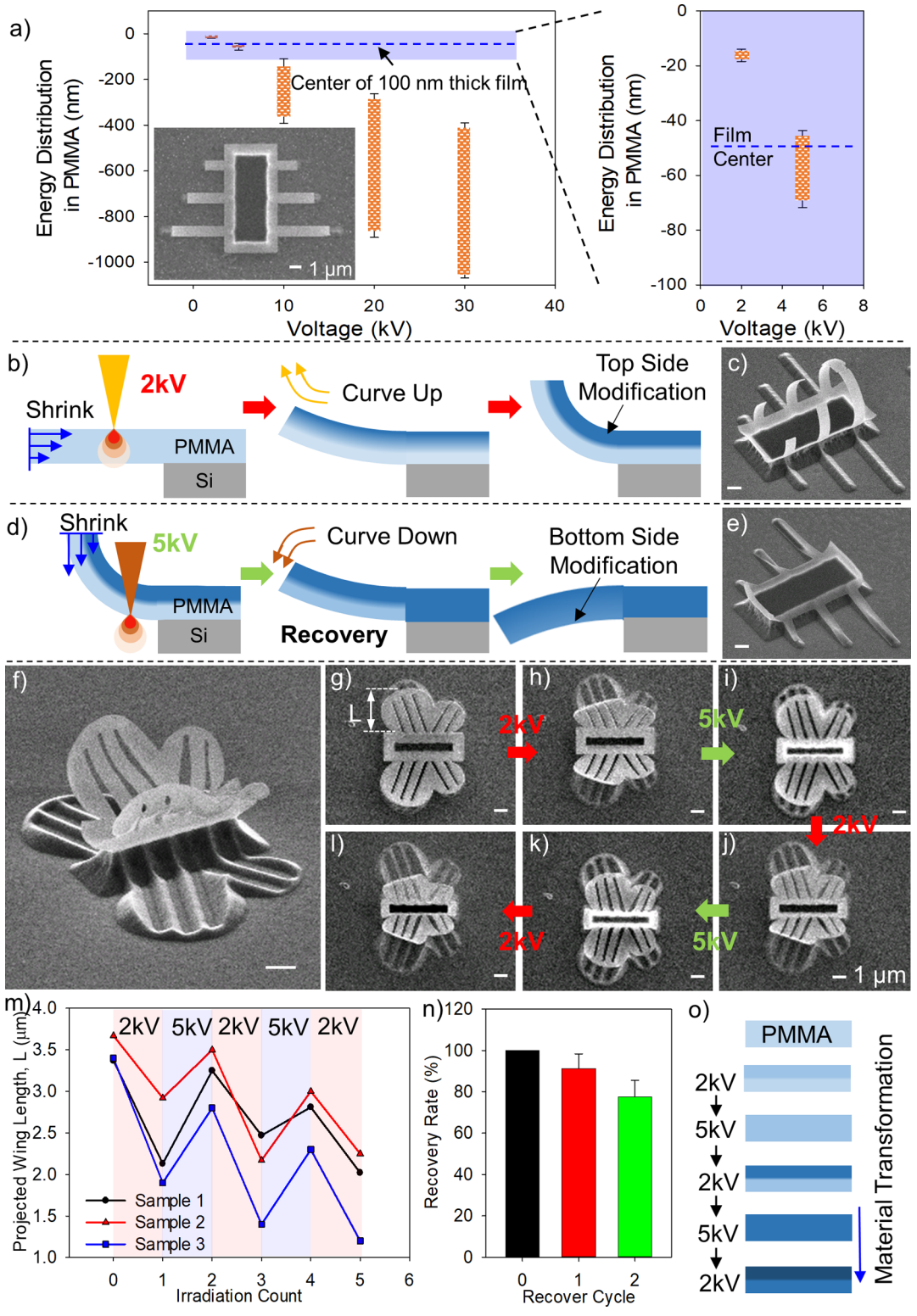

Figure 5. Reversible self-assembly achieved via tuning the irradiation voltage. (a) Monte Carlo simulation of the hotspot of energy distribution (90%) of irradiation in the PMMA thin films. (b–e) The irradiation with different voltages triggers maximum contraction in different depths of the PMMA layer, leading to different folding directions. (b) Schematics and (c) SEM image showing the upward folding of a suspended PMMA pattern under 2 keV electron irradiation. (d) Schematics and (e) SEM image showing the unfolding of the PMMA pattern by increasing the beam voltage to 5 kV. (f–l) Reversible assembly demonstrated on a butterfly PMMA pattern. The e-beam irradiation is conducted at the imaging magnitude of 1000×, which has an irradiation area of ∼100 × 80 μm. (m, n) The reversibility is measured and analyzed based on the projected wing length. (o) An explanation of the reduced reversibility is proposed based on the consummation of the polymer material.

that is perpendicular to the incident electron stream, the top surfaces of the unfolded cantilevers are exposed to the electrons again and refold upward (Figure 4d, j, k). This fold, unfold, and refold process shows a basic cycle of

https://dx.doi.org/10.1021/acs.nanolett.0c04723
Nano Lett. 2021, 21, 2066−2073

reversible assembly. However, each step of this reversible assembly process requires sample rotation and focus calibration, which is complicated and time-consuming. In addition, the unfolding process is significantly restricted by the rotation angle. A substrate that does not allow large angle rotation is not eligible for this reversible assembly. Therefore, a delicate and widely applicable reversible assembly strategy is preferred.

Driven by the need for a simple and widely applicable process, we developed the second strategy for reversible assembly. This strategy involves tuning the e-beam voltage to adjust the location of peak energy absorption along the depth of a PMMA layer (Figure 5). Depending on this location, the 2D structures are curved upward or downward, creating a reversible assembly process. Specifically, the depth distribution of absorbed energy in the polymer thin film directly affects the intensity of irradiation−polymer interaction and further determines the extent of shrinkage. Thus, a systematic understanding of electron trajectory and energy distribution is required to precisely estimate the location of shrinkage in the PMMA films. To achieve this information, Monte Carlo simulation was carried out using Casino (version 2.5.1.0) (Figure S2). The variation of electron energy (beam voltage) results in different electron implantation profiles; the depth of the hotspot is considered to be the location of 90% absorbed energy (Figures 5a and S2). The tunable depth of the hotspot provides a possibility of realizing reversible self-curving by controlling the position of the shrinkage along the depth of a PMMA layer. The localized shrinkage generates a stress gradient in the film, resulting in the deformation of the structure for self-assembly. Furthermore, the maxima of absorbed energy is not right on the surface but tens to hundreds of nanometers deep away from the surface of the PMMA film, depending on the voltage of incident electrons (Figure S2b, d, f, h, j). The peak position of the absorbed energy can be modified by tuning the electron energy (Figure 5a), which offers the possibility to program the shrinkage and stress across the depth of the PMMA layer. This means that the curving direction can be modified by positioning the maxima of absorbed energy near the top (Figure 5b, c) or the bottom of the PMMA layer (Figure 5d, e). To confirm the feasibility of this strategy, a set of suspended 100 nm thick PMMA cantilevers was fabricated through an EBL patterning process and reactive ion etching (RIE) releasing process. Because the film thickness is around 100 nm, electron irradiations with voltages of 2 and 5 kV were selected so that the maxima of absorbed energy are located in the upper and lower half of the thin film for the 2 and 5 kV settings, respectively (Figures 5a, S2). The electrons with voltage of 2 kV show a peak energy absorption at ∼−18 nm away from the top of the PMMA layer (Figure 5a); this induces shrinkage and tensile stress on the upper part of a PMMA thin film and creates upward curving away from the substrate (Figure 5b, c). On the other hand, the maximum of absorbed energy for electrons with voltage of 5 kV is located at the depth of −60 nm (Figures 5a, S2), generating shrinkage and tensile stress in the lower half of the PMMA film and creating downward curving toward the substrate (Figure 5d, e). This test result confirms the capability to control the assembly (curving) direction by tuning the depth of the maximum absorbed energy from irradiation, which provides a fundamental principle for reversible self-assembly.

To demonstrate the reversible self-assembly process, a 100 nm thick butterfly PMMA pattern (wing of a butterfly) was formed on the Si wafer by the aforementioned EBL process. Next, the pattern was partially released by etching silicon under the pattern using an RIE system. The e-beam voltage was switched between 2 and 5 kV for reversible assembly. The alternation of the e-beam voltage shifts the depth of the absorbed energy peaks between −18 and −60 nm (Figure 5a). In response to the shift of the depth, the wings of the butterfly curved upward and downward repeatedly (Figure 5f–l), mimicking the movement of the butterfly's wings while flying. The status of the wings was characterized based on the projected length of the wings (L in Figure 5g) and plotted in Figure 5m. A clear deformation and recovery trend was observed from the wave-shape graph (Figure 5m), which is a distinct behavior of a reversible process. The fast (from a few to tens of seconds) and real-time monitored reversible process that can be easily integrated with e-beam systems aligns well with the needs for exploration of small-scale soft robotics or machines. However, the curved wings do not recover by 100% to their original state. It is obvious that the recovery rate (%) is decreasing as more irradiation cycles are applied (Figure 5n). The first cycle in this reversible assembly process has a recovery rate of almost 90%; this value is decreased to around 75% for the second cycle. This behavior is attributed to the consumption of the material through cross-linking and outgassing (Figure 5o) along with each additional irradiation cycle. Especially, the PMMA near the top surface is continuously being exposed and shrinking even during the recovery process. As there is no relaxation mechanism in this reversible self-assembly, the strain induced in the upper surface is always increasing, which becomes more and more difficult to be compensated by tuning the irradiation focus to the bottom. As the folding angle (curvature radius) is determined by the induced strain difference,[33] the uncompensated strain on the top surface reduces the structure's ability to recover, leading to a decreasing recovery rate. To overcome this limitation, relaxation processes that can fully transfer the irradiated PMMA to its original state are needed. A previous study demonstrated a 100% recovery rate in cross-linked PMMA based on spontaneous or heat induced relaxation.[28] However, these mechanisms require long cure time (up to more than a week) or an additional heat source that can hardly be integrated for the in situ process in e-beam systems. Therefore, further understanding of the e-beam induced material phase change is still required to improve this reversible self-assembly process. Even with current recovery limitations, it still can find various applications where only a few precise motions are required. For example, it could serve as the in situ manipulator in the beam systems to align the nanomaterial, induce localized stress, or shield the e-beam as a nanoscale smart cover.

In conclusion, an in situ monitored reversible self-assembly methodology was developed using electron irradiation to generate stress in a single polymer layer. Under the electron irradiation, PMMA undergoes significant shrinkage as the absorbed energy induces chain scission and subsequent outgassing. The depth of the peak energy absorbed in the polymer film can be tuned by the e-beam voltage. This enables stress generation in a desired depth of the polymer layer, which controls the direction of self-curving. By repeatedly alternating the e-beam voltage, a reversible 3D self-assembly process has been demonstrated in the structured single PMMA film. In addition, combined with the naturally encoded sequence and

https://dx.doi.org/10.1021/acs.nanolett.0c04723
Nano Lett. 2021, 21, 2066−2073

localization of e-beams, the locomotion of each section in a PMMA pattern can be precisely programmed, leading to desired topology of self-assembled 3D polymer architecture. This study of the mechanisms and effective factors of irradiation-induced PMMA shrinkage and subsequent assembly not only lays a solid foundation to the fabrication of complex 3D polymer architectures, but also opens the possibility to the building of micro- and nanoscale soft robots.

■ ASSOCIATED CONTENT

Supporting Information

The Supporting Information is available free of charge at https://pubs.acs.org/doi/10.1021/acs.nanolett.0c04723.

Additional information about PMMA pillar fabrication and irradiation induced shrinkage; localized shrinkage in continuous PMMA patterns; fabrication of 2D PMMA pattern and irradiation triggered self-assembly; and electron trajectory and absorbed energy in PMMA (PDF)

■ AUTHOR INFORMATION

Corresponding Author

Jeong-Hyun Cho − *Department of Electrical and Computer Engineering, University of Minnesota, Minneapolis, Minnesota 55455, United States;* orcid.org/0000-0003-2870-1960; Email: jcho@umn.edu

Author

Chunhui Dai − *Department of Electrical and Computer Engineering, University of Minnesota, Minneapolis, Minnesota 55455, United States*

Complete contact information is available at: https://pubs.acs.org/10.1021/acs.nanolett.0c04723

Notes

The authors declare no competing financial interest.

■ ACKNOWLEDGMENTS

This research was supported by the National Science Foundation under Grant CMMI-1454293. Portions of this work were conducted in the Minnesota Nano Center, which is supported by the National Science Foundation through the National Nano Coordinated Infrastructure Network (NNCI) under Award ECCS-2025124. This work was supported partially by the National Science Foundation through the University of Minnesota MRSEC under Award DMR-2011401. Part of this work was carried out in the College of Science and Engineering Characterization Facility, University of Minnesota, which has received capital equipment funding from the National Science Foundation through the UMN MRSEC under Award DMR-2011401. C.D. acknowledges support from the Doctoral Dissertation Fellowship from the University of Minnesota.

■ REFERENCES

(1) Wang, X.; Dong, K.; Choe, H. S.; Liu, H.; Lou, S.; Tom, K. B.; Bechtel, H. A.; You, Z.; Wu, J.; Yao, J. Multifunctional microelectro-opto-mechanical platform based on phase-transition materials. *Nano Lett.* **2018**, *18*, 1637−1643.

(2) Xu, S.; Yan, Z.; Jang, K. I.; Huang, W.; Fu, H.; Kim, J.; Wei, Z.; Flavin, M.; McCracken, J.; Wang, R.; Badea, A.; Liu, Y.; Xiao, D.; Zhou, G.; Lee, J.; Chung, H. U.; Cheng, H.; Ren, W.; Banks, A.; Li, X.; Paik, U.; Nuzzo, R. G.; Huang, Y.; Zhang, Y.; Rogers, J. A. Materials science. Assembly of micro/nanomaterials into complex, three-dimensional architectures by compressive buckling. *Science* **2015**, *347*, 154−159.

(3) Fu, H.; Nan, K.; Bai, W.; Huang, W.; Bai, K.; Lu, L.; Zhou, C.; Liu, Y.; Liu, F.; Wang, J. Morphable 3D mesostructures and microelectronic devices by multistable buckling mechanics. *Nat. Mater.* **2018**, *17*, 268−276.

(4) Must, I.; Kaasik, F.; Poldsalu, I.; Mihkels, L.; Johanson, U.; Punning, A.; Aabloo, A. Ionic and capacitive artificial muscle for biomimetic soft robotics. *Adv. Eng. Mater.* **2015**, *17*, 84−94.

(5) Miskin, M. Z.; Dorsey, K. J.; Bircan, B.; Han, Y.; Muller, D. A.; McEuen, P. L.; Cohen, I. Graphene-based bimorphs for micron-sized, autonomous origami machines. *Proc. Natl. Acad. Sci. U. S. A.* **2018**, *115*, 466−470.

(6) Randhawa, J. S.; Keung, M. D.; Tyagi, P.; Gracias, D. H. Reversible actuation of microstructures by surface chemical modification of thin film bilayers. *Adv. Mater.* **2010**, *22*, 407−410.

(7) Na, J.; Evans, A. A.; Bae, J.; Chiappelli, M. C.; Santangelo, C. D.; Lang, R. J.; Hull, T. C.; Hayward, R. C. Programming reversibly self-folding origami with micropatterned photo-crosslinkable polymer trilayers. *Adv. Mater.* **2015**, *27*, 79−85.

(8) Jamal, M.; Zarafshar, A. M.; Gracias, D. H. Differentially photo-crosslinked polymers enable self-assembling microfluidics. *Nat. Commun.* **2011**, *2*, 1−6.

(9) Miskin, M. Z.; Cortese, A. J.; Dorsey, K.; Esposito, E. P.; Reynolds, M. F.; Liu, Q.; Cao, M.; Muller, D. A.; McEuen, P. L.; Cohen, I. Electronically integrated, mass-manufactured, microscopic robots. *Nature* **2020**, *584*, 557−561.

(10) Seminara, A.; Pokroy, B.; Kang, S. H.; Brenner, M. P.; Aizenberg, J. Mechanism of nanostructure movement under an electron beam and its application in patterning. *Phys. Rev. B: Condens. Matter Mater. Phys.* **2011**, *83*, 235438.

(11) Rajput, N. S.; Le Marrec, F.; El Marssi, M.; Jouiad, M. Fabrication and manipulation of nanopillars using electron induced excitation. *J. Appl. Phys.* **2018**, *124*, 074301.

(12) Chalapat, K.; Chekurov, N.; Jiang, H.; Li, J.; Parviz, B.; Paraoanu, G. Self-organized origami structures via ion induced plastic strain. *Adv. Mater.* **2013**, *25*, 91−95.

(13) Dai, C.; Cho, J. In situ monitored self-assembly of three-dimensional polyhedral nanostructures. *Nano Lett.* **2016**, *16*, 3655−3660.

(14) Supekar, O.; Brown, J.; Eigenfeld, N.; Gertsch, J.; Bright, V. Atomic layer deposition ultrathin film origami using focused ion beams. *Nanotechnology* **2016**, *27*, 49LT02.

(15) Pan, R.; Li, Z.; Liu, Z.; Zhu, W.; Zhu, L.; Li, Y.; Chen, S.; Gu, C.; Li, J. Rapid bending origami in micro/nanoscale toward a versatile 3D metasurface. *Laser Photonics Rev.* **2020**, *14*, 1900179.

(16) Dai, C.; Agarwal, K.; Cho, J. Ion-Induced Localized Nanoscale Polymer Reflow for Three-Dimensional Self-Assembly. *ACS Nano* **2018**, *12*, 10251−10261.

(17) Liu, J.; Xu, J.; Ni, Y.; Fan, F.; Zhang, C.; Yu, S. A family of carbon-based nanocomposite tubular structures created by in situ electron beam irradiation. *ACS Nano* **2012**, *6*, 4500−4507.

(18) Jiang, Z.; He, J.; Deshmukh, S. A.; Kanjanaboos, P.; Kamath, G.; Wang, Y.; Sankaranarayanan, S. K.; Wang, J.; Jaeger, H. M.; Lin, X. Subnanometre ligand-shell asymmetry leads to Janus-like nanoparticle membranes. *Nat. Mater.* **2015**, *14*, 912−917.

(19) Dai, C.; Li, L.; Wratkowski, D.; Cho, J. H. Electron irradiation driven nanohands for sequential origami. *Nano Lett.* **2020**, *20*, 4975−4984.

(20) Dai, C.; Lin, Z.; Agarwal, K.; Mikhael, C.; Aich, A.; Gupta, K.; Cho, J. H. Self-assembled 3D nano-split rings for plasmon-enhanced optofluidic sensing. *Nano Lett.* **2020**, *20*, 6697−6705.

(21) Dai, C.; Joung, D.; Cho, J. Plasma triggered grain coalescence for self-assembly of 3D nanostructures. *Nano-Micro Lett.* **2017**, *9*, 27.

(22) Rykaczewski, K.; Hildreth, O. J.; Wong, C. P.; Fedorov, A. G.; Scott, J. H. J. Guided three-dimensional catalyst folding during metal-assisted chemical etching of silicon. *Nano Lett.* **2011**, *11*, 2369−2374.

(23) Liu, Z.; Du, S.; Cui, A.; Li, Z.; Fan, Y.; Chen, S.; Li, W.; Li, J.; Gu, C. High quality factor mid-infrared toroidal excitation in folded 3D metamaterials. *Adv. Mater.* **2017**, *29*, 1606298.
(24) Mao, Y.; Zheng, Y.; Li, C.; Guo, L.; Pan, Y.; Zhu, R.; Xu, J.; Zhang, W.; Wu, W. Programmable bidirectional folding of metallic thin films for 3D chiral optical antennas. *Adv. Mater.* **2017**, *29*, 1606482.
(25) Liu, Z.; Du, H.; Li, J.; Lu, L.; Li, Z.; Fang, N. X. Nano-kirigami with giant optical chirality. *Sci. Adv.* **2018**, *4*, eaat4436.
(26) Kim, T.; Jeong, H. E.; Suh, K. Y.; Lee, H. H. Stooped nanohairs: geometry-controllable, unidirectional, reversible, and robust gecko-like dry adhesive. *Adv. Mater.* **2009**, *21*, 2276−2281.
(27) Giambastiani, D.; Dispinzeri, F.; Colangelo, F.; Forti, S.; Coletti, C.; Tredicucci, A.; Pitanti, A.; Roddaro, S. Stress−strain in electron-beam activated polymeric micro-actuators. *J. Appl. Phys.* **2020**, *128*, 115104.
(28) Colangelo, F.; Pitanti, A.; Mišeikis, V.; Coletti, C.; Pingue, P.; Pisignano, D.; Beltram, F.; Tredicucci, A.; Roddaro, S. Controlling local deformation in graphene using micrometric polymeric actuators. *2D Mater.* **2018**, *5*, 045032.
(29) Wu, C. L.; Li, F. C.; Pao, C. W.; Srolovitz, D. J. Folding sheets with ion beams. *Nano Lett.* **2017**, *17*, 249−254.
(30) Lee, E.; Rao, G.; Mansur, L. LET effect on cross-linking and scission mechanisms of PMMA during irradiation. *Radiat. Phys. Chem.* **1999**, *55*, 293−305.
(31) Yasuda, M.; Furukawa, Y.; Kawata, H.; Hirai, Y. Multiscale simulation of resist pattern shrinkage during scanning electron microscope observations. *J. Vac. Sci. Technol., B: Nanotechnol. Microelectron.: Mater., Process., Meas., Phenom.* **2015**, *33*, 06FH02.
(32) Azuma, T.; Chiba, K.; Abe, H.; Motoki, H.; Sasaki, N. Mechanism of ArF resist-pattern shrinkage in critical-dimension scanning electron microscopy measurement. *J. Vac. Sci. Technol., B: Microelectron. Process. Phenom.* **2004**, *22*, 226−230.
(33) Tian, Z.; Xu, B.; Hsu, B.; Stan, L.; Yang, Z.; Mei, Y. Reconfigurable vanadium dioxide nanomembranes and microtubes with controllable phase transition temperatures. *Nano Lett.* **2018**, *18*, 3017−3023.

https://dx.doi.org/10.1021/acs.nanolett.0c04723
Nano Lett. 2021, 21, 2066−2073